Exact mean field concept to compute defect energetics in random alloys on rigid lattices

G. Bonny, N. Castin, M.I. Pascuet, Y. Çelik

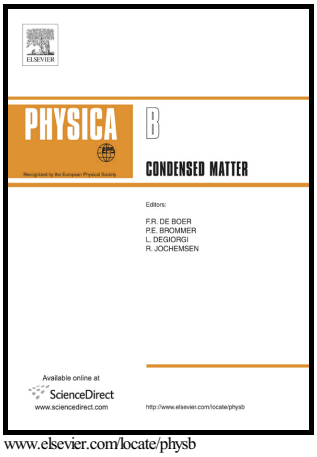

www.elsevier.com/locate/physb

PII: S0921-4526(17)30217-X
DOI: http://dx.doi.org/10.1016/j.physb.2017.04.032
Reference: PHYSB309923

To appear in: *Physica B: Physics of Condensed Matter*

Received date: 10 February 2017
Revised date: 24 April 2017
Accepted date: 29 April 2017

Cite this article as: G. Bonny, N. Castin, M.I. Pascuet and Y. Çelik, Exact mean field concept to compute defect energetics in random alloys on rigid lattices *Physica B: Physics of Condensed Matter* http://dx.doi.org/10.1016/j.physb.2017.04.032

Exact mean field concept to compute defect energetics in random alloys on rigid lattices

G. Bonny[1*], N. Castin[1], M.I. Pascuet[1,2], Y. Çelik[1]

[1]SCK•CEN, Boeretang 200, B-2400 Mol, Belgium

[2]CNEA-CONICET, Godoy Cruz 2290, (C1425FQB) CABA, Argentina

[*]Corresponding author. giovanni.bonny@gmail.com

Abstract

In modern materials science modeling, the evolution of the energetics of random alloys with composition are desirable input parameters for several meso-scale and continuum scale models. When using atomistic methods to parameterize the above mentioned concentration dependent function, a mean field theory can significantly reduce the computational burden associated to obtaining the desired statistics in a random alloy. In this work, a mean field concept is developed to obtain the energetics of point-defect clusters in perfect random alloys. It is demonstrated that for a rigid lattice the concept is mathematically exact. In addition to the accuracy of the presented method, it is also computationally efficient as a small box can be used and perfect statistics are obtained in a single run. The method is illustrated by computing the formation and binding energy of solute and vacancy pairs in FeCr and FeW binaries. In addition, the dissociation energy of small vacancy clusters was computed in FeCr and FeCr-2%W alloys, which are considered model alloys for Eurofer steels. As a result, it was concluded that the dissociation energy is not expected to vary by more than 0.1 eV in the 0-10% Cr and 0-2% W composition range. The present mean field concept can be directly applied to parameterize meso-scale models, such as cluster dynamics and object kinetic Monte Carlo models.

Keywords: atomistic modelling; random alloys; rigid lattice

1. Introduction

In modern materials science modeling, the evolution of the energetics of random alloys with composition are desirable input parameters for several meso-scale and continuum scale models. On the continuum scale, several thermodynamic packages (MatCalc, ThermoCalc, FactSage…) [1-3] hinge on an accurate description of the free energy of random solid solution, even outside their experimental stability range. On the meso-scale, cluster dynamics models [4] and object kinetic Monte Carlo methods [5-7] hinge on an accurate description of

the formation, binding and dissociation energy of point-defects and point-defect clusters. Here solutes and solute clusters are also considered as point-defect (clusters).

When using atomistic methods to parameterize the above mentioned concentration dependent function, a mean field theory (MFT) can significantly reduce the computational burden associated to obtaining the desired statistics in a random alloy. In a density functional theory (DFT) framework, the coherent potential approximation (CPA) [8] is a well-established method to obtain the energetics of the random alloy in a given supercell.

In the framework of empirical interatomic potentials, Smith and Was developed a first order MFT approximation in the form of an effective atom method [9] such that the alloy becomes an aggregate of identical effective atoms. Later, Bonny et al refined the method by introducing higher order corrections in the form of a so-called variance expansion, for both binary [10] and multi-component alloys [11]. These techniques were successfully applied to estimate, for example, mixing enthalpy, stacking fault energy, elastic constants and friction stress [10-13] in concentrated random solid solutions.

In the framework of rigid lattices, an MFT is realized by the Bragg-Williams-Gorsky point approximation [14, 15] and is an excellent tool to obtain the energetics of random solid solutions. The latter assumes that the occupancy of all lattice sites are uncorrelated and the theory is well developed for perfect lattice crystals. However, for lattice configurations (supercells) containing point-defects and point-defect clusters, for example vacancies and solute atoms, the theory is not well developed.

In this work this MFT concept is further developed to obtain the energetics (formation and binding energy) of point-defect (clusters) embedded in random solid solutions. Moreover, we will prove that the developed MFT for the rigid lattice is mathematically exact. The MFT is illustrated using a recently developed clusters expansion (CE) for the FeCrW-vacancy (v) system [16, 17]. The latter serves as a model alloy for reduced activation steels, such as Eurofer, that are considered for structural components in future fusion devices [18].

The evolution with composition of the formation and binding energy of various v-solute and solute-solute pairs in random solid solutions is calculated. In addition, the stability of small vacancy clusters in random FeCr alloys containing up to 2% W is computed.

2. Methods

The configurational energy per atom of a given lattice configuration is easily described by a so-called cluster expansion (CE) [19, 20],

$$E(\boldsymbol{\sigma}) = J_0 + \sum_{\alpha \subseteq \alpha_{\max}} \sum_{\boldsymbol{s}} m_\alpha J_\alpha^{\boldsymbol{s}} \, \xi_\alpha^{\boldsymbol{s}}(\boldsymbol{\sigma}). \quad (1)$$

Here α runs over all symmetrically inequivalent clusters contained in the maximum cluster $\alpha_{\max}$ that contains all physical interactions. The vector $\boldsymbol{\sigma} = (\sigma_1, \ldots, \sigma_N)$ specifies the species on each of the N number of lattice positions. For a K-element alloy, the summation over the decoration variable $\boldsymbol{s} = (s_1, \ldots, s_{|\alpha_{\max}|})$ runs over all possible permutations, where s_i can take the values 1,…, K-1. The effective cluster interactions (ECI) are denoted by $J_\alpha^{\boldsymbol{s}}$ and the number of equivalent clusters α per lattice site are denoted by the multiplicity factor m_α.

The cluster correlation functions $\xi_\alpha^{\boldsymbol{s}}(\boldsymbol{\sigma})$ are defined as,

$$\xi_\alpha^{\boldsymbol{s}}(\boldsymbol{\sigma}) = \langle \prod_{i=1}^{|\alpha|} \phi_{s_i}(\sigma_i) \rangle_\alpha, \quad (2)$$

where the average runs over all symmetry equivalent clusters and ϕ_{s_i} are the so-called configuration functions, which serve as basis functions to span the K^N configurational space (see [19, 20] for more details).

To illustrate the method developed in Section 3, the recently developed CE for the quaternary FeCrWv system [17] is applied. For this CE, K=4 and the site operator σ_n takes the values -1, 0, +1, +2 if site n is occupied by Cr, v, Fe or W, respectively. The configuration functions are defined as $\phi_0 = 1$, $\phi_1 = \sigma_n$, $\phi_1 = \sigma_n^2$ and $\phi_1 = \sigma_n^3$.

3. Mean field theory

The computation of the formation energy of a defect, or the binding energy between defects, in a random alloy is a challenging task due to the scatter introduced by the stochasticity of the random alloys. In a box containing N atoms and a defect D containing N_D atoms/vacancies the formation energy, E_f, is given as,

$$E_f(D) = N\,E(D) - (N - N_D)E_{\text{ref}}(M) - N_D\,E_{\text{ref}}(D). \quad (3)$$

Here $E(D)$ denotes the average energy per atom of the configuration containing the defect, while $E_{\text{ref}}(M)$ and $E_{\text{ref}}(D)$ denote the average energy per atom for the reference state of the

matrix and defect, respectively. Here the reference state for M is the defect free random alloy while the reference state for D is bcc Fe, Cr, W or vacuum (E_{ref}(v)=0).

The total binding energy, E_{b}, between R defects D_i is given as,

$$E_{\mathrm{b}}(D_1, \dots, D_R) = \sum_{i=1}^{R} E_{\mathrm{f}}(D_i) - E_{\mathrm{f}}(D_1, \dots, D_R), \tag{4}$$

where positive values indicate attraction and negative ones repulsion.

Every energy calculation in the random alloy has a statistical error, and as shown in equations 3 and 4, this error accumulates when computing E_{f} and E_{b}. This error accumulation can be (partially) reduced by computing the formation energy in boxes containing special quasi-random structures (SQSs) [21] and by averaging E_{f} over many different SQSs or random configurations. However, given that the standard error decreases with the inverse of the square root of the number of trials, many calculations are necessary.

In this section we propose an MFT to compute the energy of a supercell containing a defect in a random alloy. The method is based on the BWG point approximation and replaces the lattice positions occupied by random atoms by a grey alloy. As shown below, for a rigid lattice model this approximation is exact. The proof goes as follows: the average over all different random configurations for the correlation functions can be written as,

$$\begin{aligned} \langle \xi_\alpha^s(\sigma) \rangle_{\mathrm{rand}} &= \langle \langle \textstyle\prod_{i=1}^{|\alpha|} \phi_{s_i}(\sigma_i) \rangle_{\mathrm{rand}} \rangle_\alpha \\ &= \langle \langle \textstyle\prod_i' \phi_{s_i}(\sigma_i) \rangle_{\mathrm{rand}} \langle \textstyle\prod_i'' \phi_{s_i}(\sigma_i) \rangle_{\mathrm{rand}} \rangle_\alpha \\ &= \langle \textstyle\prod_i' \phi_{s_i}(\sigma_i) \ \prod_i'' \langle \phi_{s_i}(\sigma_i) \rangle_{\mathrm{rand}} \rangle_\alpha \\ &= \langle \textstyle\prod_i' \phi_{s_i}(\sigma_i) \ \prod_i'' \xi_1^{s_i}(x) \rangle_\alpha . \end{aligned} \tag{5}$$

In the first line we switched the average over equivalent clusters with the average over the random configurations; in the second line we split up the product over the cluster sites depending on the occupying species: Π_i', runs over the cluster sites that are occupied by the defected atoms while Π_i'' runs over the cluster sites that form the alloyed background. In the third line we used the fact that the product Π_i' yields a constant factor independent of the alloyed background and the fact that the sites in a random alloy are uncorrelated, thereby moving the average over the random configurations inside the product Π_i''. In the last line we remark that the average of the different configurations of the occupation functions is exactly the point correlation function $\xi_1^{s_i}(x)$ for the given concentration vector $x = (x_1, \dots, x_K)$.

As shown in [22], there is a linear relationship between the concentration vector (point probabilities) and the point correlation functions. For our FeCrWv system the relations are given as,

$$\begin{cases} \xi_1^{(0)} = x_{\mathrm{Fe}} + x_{\mathrm{Cr}} + x_{\mathrm{Vac}} + x_{\mathrm{W}} = 1 \\ \xi_1^{(1)} = x_{\mathrm{Fe}} - x_{\mathrm{Cr}} + 2\,x_{\mathrm{W}} \\ \xi_1^{(2)} = x_{\mathrm{Fe}} + x_{\mathrm{Cr}} + 4\,x_{\mathrm{W}} \\ \xi_1^{(3)} = x_{\mathrm{Fe}} - x_{\mathrm{Cr}} + 8\,x_{\mathrm{W}} \end{cases} . \tag{6}$$

The last equality in equation 6 is nothing more than a mean field approximation, that embeds the defect configuration into a grey alloy. However, given the linear relation between the energy and the correlation functions for a CE, this MFT is exact. Because of the accuracy of this concept, details in E_f and E_b with composition are visible that would be computationally unaffordable with the traditional methods (see Section 4).

4. Results

The results presented in this section were obtained by applying the MFT presented in Section 3. All calculations were performed in the smallest possible simulation box that complies with the minimum image condition, i.e., maximum distance of the defect augmented by twice the maximum cluster size used in the CE. For a compact v_{15} cluster, this leads to a bcc supercell of dimensions 5×5×5 a_0^3 containing 250 atoms. Although this box is small, it is equivalent to embedding the defect in an infinite random alloy with perfect statistics.

As a starting point we present the mixing enthalpy of both FeCr and FeW binaries in the top panel of Fig. 1. The mixing enthalpy is defined as the formation energy per atom of the corresponding alloy. As already extensively discussed in [17], both curves reproduce the available DFT data well, characterized by an inversion of curvature and negative heat of mixing in the Fe-rich limit. In the bottom panel of Fig. 1, E_f of an Fe/Cr atom and an Fe/W atom in the FeCr and FeW binaries is presented, respectively.

Consistent with the mixing enthalpy, both E_f of Cr and W are slightly negative in Fe. Then, with the alloying of Cr/W it becomes positive and converges to zero in the limit of pure Cr and W, respectively. Indeed, following the definition of E_f (see equation 4), E_f of the host solute atom becomes zero in the host. E_f of Fe in both W and Cr is positive, with the value in

W larger than the one in Cr. This is fully consistent with the slope of the mixing enthalpy at the W/Cr rich side.

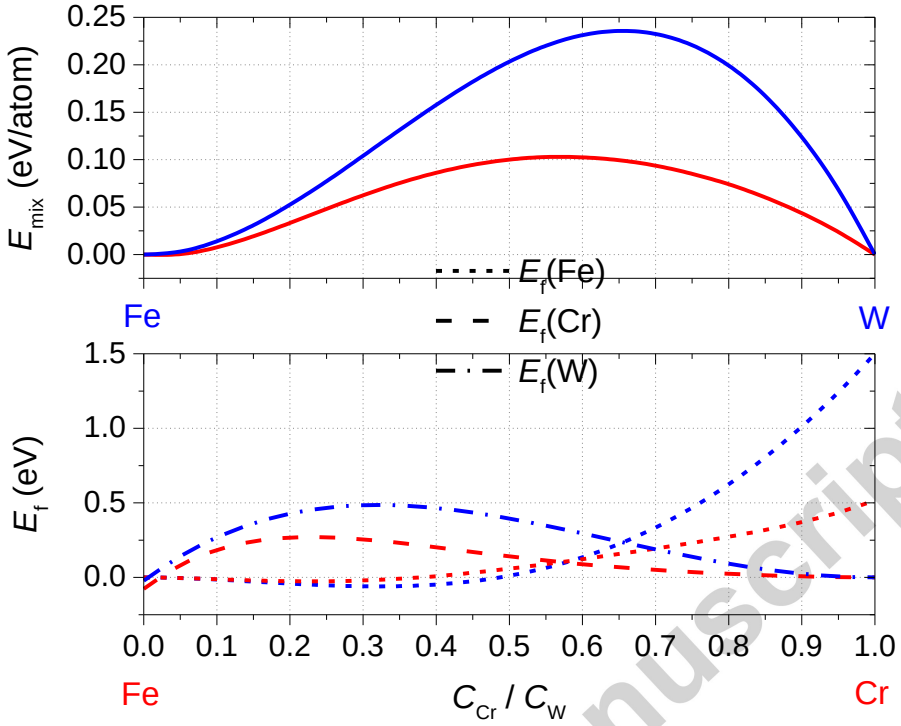

Fig. 1 – Mixing enthalpy (top panel) and formation energy (bottom panel) of a solute atom in FeCr and FeW binaries.

In Fig. 2 E_b between solute-solute and solute-v pairs in the FeCr and FeW binaries is plotted. For Cr-Cr pairs in the FeCr binary, repulsion is observed up to ~15% Cr, above which the interaction becomes attractive and converges to zero in pure Cr. The change of sign of the Cr-Cr interaction is consistent with the interaction parameters derived in [23, 24] based on the experimental observation of short range order (SRO).

Indeed, both experiments [23, 24] and atomistic simulations [25] predict a negative SRO parameter below 10-15% Cr and positive above, with the precise cross over point depending on the annealing time [25]. The appearance of the observed SRO at low Cr content and precipitation at high Cr content [26-28] is a consequence of the change of sign and curvature of the mixing enthalpy, a feature that is well reproduced by the present CE.

For W-W pairs the cross over only appears at ~30% W. The repulsive W-W interactions is consistent with a tendency long range order (LRO). Indeed, the alloying of Fe with W leads to the formation of the Laves and μ-intermetallic phases [29].

For both FeCr and FeW binaries, E_b of v-Fe, v-W and v-Cr pairs were investigated. E_b between v-W and v-Cr pairs exhibit similar behavior: attractive interaction up to ~40% Cr/W, and repulsive above; eventually converging to zero in pure Cr and W, respectively. We note that for the FeCr case, there is a shallow maximum around 10% Cr, a subtle feature that is likely to be lost in standard statistical calculations.

In both FeCr and FeW binaries, the E_b of v-Fe pairs are attractive in the W- and Cr-rich limit and reduce to essentially zero around 60% Fe.

E_b of Fe-Fe pairs in both the FeCr and FeW binaries is positive, with the largest value in the FeW binary. This observation is consistent with the slope of the mixing enthalpy in the Cr and W rich limit.

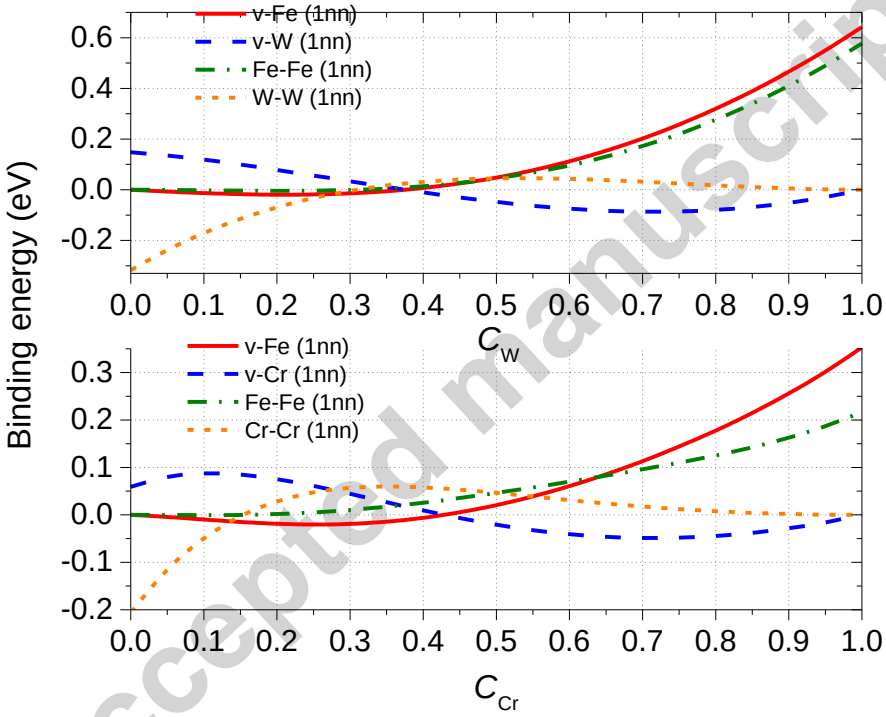

Fig. 2 – Binding energy of solute pairs in FeW (top panel) and FeCr (bottom panel) binaries.

In Fig. 3 the evolution with composition of E_b between 1nn and 2nn v-v pairs in FeCr and FeW binaries is given. In pure Fe, the CE predicts the 2nn di-vacancy as most stable configuration, consistent with DFT calculations (see [17] and references therein). In pure W and Cr, on the other hand, the 1nn di-vacancy is the most stable, although the actual values and even sign is open for debate following the different DFT data sets (see [17] and references therein).

The evolution of E_b of the 1nn and 2nn di-vacancy differs essentially. For the 1nn pair, the evolution in the FeCr and FeW binaries is similar, characterized by a deep (negative) minimum around 55% Cr/W. Thus, the 1nn di-vacancy is only stable in the ranges 0-25% and 85%-100% W, and 0-35% and 75-100% Cr. The 2nn di-vacancy remains attractive in the whole concentration range for the FeCr binary, while the one in the FeW binary becomes repulsive starting from 70% W. As a result, the 2nn di-vacancy is the most stable configuration in the range 0-70% and 0-85% W (with no stable configuration in the range 70-85% W). In the FeCr binary, the 2nn di-vacancy is the most stable configuration in the range 0-80% Cr, at which point the 1nn di-vacancy becomes the most stable configuration. The present analysis is based on subtle differences in the trends of the binding energy curves, which are likely to be lost in the statistics of traditional methods.

We note that in the 70-85% W range the CE predicts no stable di-vacancies. Given the small value of the maximum repulsion (~ -0.02 eV), it is unclear if the non-existence of a di-vacancy is physical or an artifact of the CE. For all other cases, regardless the significant repulsion of the 1nn di-vacancy, there is always a stable di-vacancy configuration.

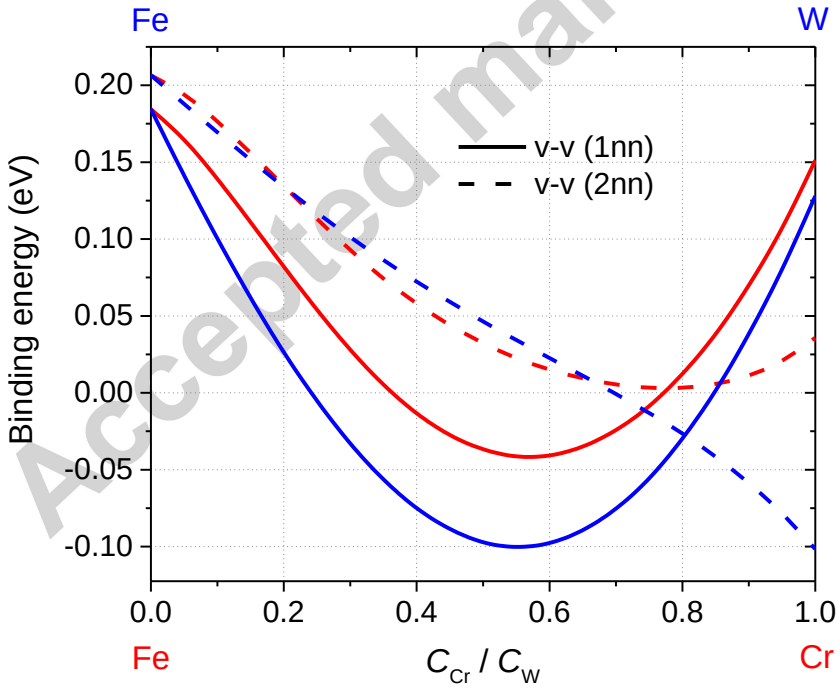

Fig. 3 – Binding energy of 1nn and 2nn vacancy pairs in the FeCr and FeW binaries.

In Fig. 4 E_f per vacancy is presented for a v, v_2, v_3, v_4, v_9 and v_{15} in FeCr alloys. For the v-clusters the most stable configurations are chosen: for v-clusters up to v_9 this is a

topology where the number of 2nn v-v pairs are maximized while for v_{15} and larger clusters this is the most compact topology. E_f for the single vacancy reduces from 2.16 eV in pure Fe to reach a minimum of 1.89 eV at 45% Cr and subsequently rises again to 2.78 eV for pure Cr.

The initial decrease of E_f for the single vacancy is consistent with the small but attractive v-Cr (~ 0.05 eV) binding predicted by DFT [30] and reproduced by the CE (see [17]). Due to the attractive interaction between a vacancy and Cr atoms in bcc Fe, E_f initially decreases.

We note that in the work by del Rio et al [31] the E_f a single vacancy remains almost constant up to ~6% (consistent with our results) but then increases monotonically with Cr concentration, contrary to our results. This discrepancy is explained by the small but repulsive v-Cr binding predicted by the used potential (~ -0.05 eV, see [32]), which is a minor descrepancy of the potential compared to the DFT data. Due to the repulsive interaction between a vacancy and Cr atoms in bcc Fe, E_f thus increases.

In addition, the comparison between Fig. 4 and figure 5 in [31] illustrates the power of our MFT: even statistics over ~1000 configurations provide large error bars compared to the infinite statistics provided by our MFT.

With increasing number of vacancies in the clusters, the E_f per vacancy reduces progressively to a constant value, consistent with classical liquid tear drop (LTD) models. The LTD model is based on the energy balance associated with a volume term and surface term (see for example [33]). Starting from v_4, the minimum around 45% becomes negligible, making E_f of the v-clusters quasi constant up to 40% Cr. The additional effect of 2% W on E_b for v-cluster is negligible.

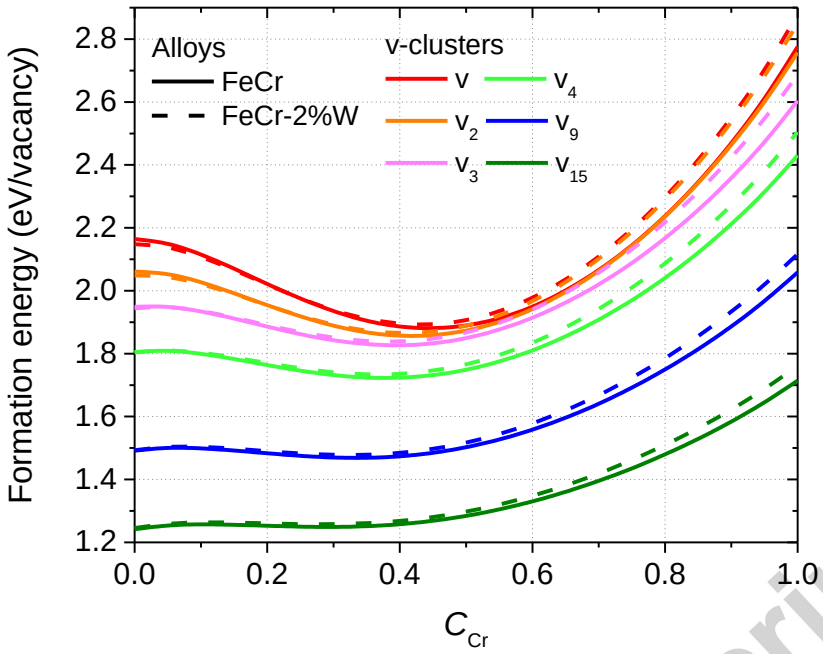

Fig. 4 – Formation energy of the most stable v-clusters for FeCr alloys with and without 2% W.

The binding energy, E_b, per vacancy and incremental binding energy, $E_b^{inc} = E_b(v_N) - E_b(v_{N-1})$, of different v-clusters in FeCr alloys is presented in Fig. 5. The latter is a measure of how strong a single v is bound to a v_N cluster and is essential in the determination of the dissociation energy. The dissociation energy, E_{diss}, is classically estimated as $E_{diss}(v_N) = E_b^{inc}(v_N) + E_m(v)$, with $E_m(v)$ the migration energy of a single v. Both types of binding energy decrease with increasing cluster size to a constant value, consistent with the LTD model. In both cases and for all cluster sizes the binding energy decreases with Cr content to a minimum between 50-60% Cr and increases back to the values in pure Cr, which are higher than in pure Fe. The addition of 2% W has a negligible influence on the either binding energy.

Thus, in the region of importance for Eurofer steels (0-15%Cr, 0-2%W), the binding energy per vacancy varies by at most 0.1 eV and remains constant with the addition of 2% W. For E_b^{inc} the same conclusions are true and thus $E_{diss}(v_N)$ is estimated to be quasi constant in the composition range relevant for Eurofer steels. Such results could serve as an input in cluster dynamics and object kinetic Monte Carlo models.

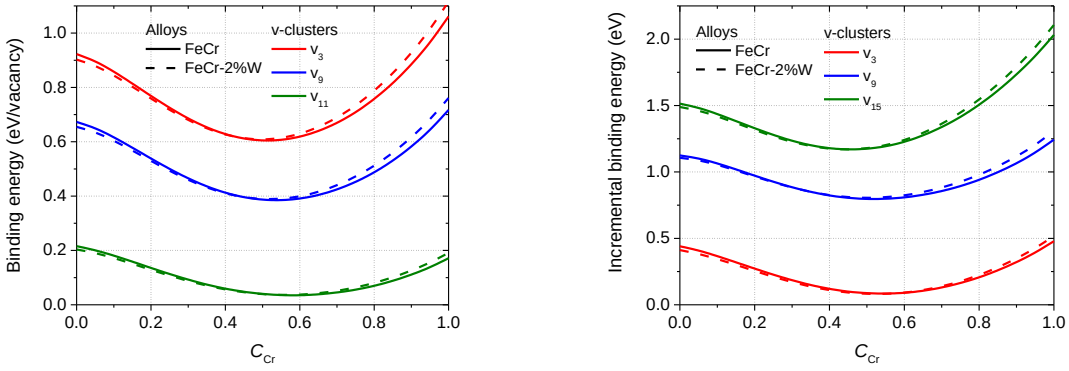

Fig. 5 – (a) Binding energy per vacancy and (b) incremental binding energy of different v-clusters in FeCr and FeCr-2%W alloys.

5. Conclusions

A mean field concept is developed to obtain the energetics of point-defect clusters in perfect random alloys. It was demonstrated that for a rigid lattice the concept is mathematically exact. In addition to the accuracy of the presented method, it is also computationally efficient as a small box can be used and perfect statistics are obtained in a single run.

The method is illustrated by computing the formation and binding energy of solute and vacancy pairs in the FeCr and FeW binaries. In addition, the dissociation energy of small vacancy clusters was estimated in FeCr and FeCr-2%W alloys, which are considered model alloys for Eurofer steels. As a result, it was concluded that the dissociation energy is not expected to vary by more than 0.1 eV in the 0-10% Cr and 0-2% W composition range.

The present mean field concept can be directly applied to parameterize meso-scale models, such as cluster dynamics and object kinetic Monte Carlo models.

Acknowledgements

This work has been carried out within the framework of the EUROfusion Consortium and has received funding from the Euratom research and training programme 2014-2018 under grant agreement No 633053. The views and opinions expressed herein do not necessarily reflect

those of the European Commission. GB acknowledges support from Mr. I.V. Bonny in preparation of the manuscript.

References

[1] E. Kozeschnik, B. Buchmayr, *MatCalc — A simulation tool for multicomponent thermodynamics, diffusion and phase transformations*, in: H. Cerjak, et al. (Eds.), Mathematical Modelling of Weld Phenomena, vol. 5, 2001, pp. 349–361.

[2] J.O. Andersson, T. Helander, L. Höglund, P.F. Shi and B. Sundman B, Calphad 26 (2202) 273.

[3] C.W. Bale, E. Bélisle, P. Chartrand, S.A. Decterov, G. Eriksson, K. Hack, I.H. Jung, Y.B. Kang, J. Melançon, A.D. Pelton, C. Robelin and S. Petersen, Calphad 33 (2009) 295.

[4] A. Hardouin-Duparc, C. Moingeon, N. Smetniansky-de-Grande and A. Barbu, J. Nucl. Mater. 302 (2002) 143.

[5] M. J. Caturla, N. Soneda, E. Alonso, B. D. Wirth, T. Diaz de la Rubia and J. M. Perlado, J. Nucl. Mater. 276 (2000) 13.

[6] C. Domain, C. S. Becquart and L. Malerba, J. Nucl. Mater. 335 (2004) 121.

[7] N. Castin, A. Bakaev, G. Bonny, A. Sand, L. Malerba and D. Terentyev, "On the onset of void swelling in pure tungsten under neutron irradiation: an object kinetic Monte Carlo approach", submitted to J. Nucl. Mater. (2016).

[8] B.L. Györffy, Phys. Rev. B 5 (1972) 2382.

[9] R.W. Smith and G.S. Was, Phys. Rev. B 40 (1989) 10322.

[10] G. Bonny, R.C. Pasianot, L. Malerba, Philos. Mag. 89 (2009) 711.

[11] G. Bonny, D. Terentyev, R.C. Pasianot, S. Poncé and A. Bakaev, Modelling Simul. Mater. Sci. Eng. 19 (2011) 085008.

[12] C. Varvenne, A. Lusque, W.G. Nöhring and W.A. Curtin, Phys. Rev. B 93 (2016) 104201.

[13] C. Varvenne, A. Lusque and W.A. Curtin, Acta Mater. 118 (2016) 1 and 164.

[14] V.S. Gorsky, J. Phys. 50 (1928) 64.

[15] W.L. Bragg and E.J. Williams, Proc. Roy. Soc. 145A (1935) 699.

[16] M.Yu. Lavrentiev, R. Drautz, D. Nguyen-Manh, T.P.C. Klaver and S.L. Dudarev, Phys. Rev. B 75 (2007) 014208.

[17] G. Bonny, N. Castin, C. Domain, P. Olsson, B. Verreyken, M. I. Pascuet and D. Terentyev, Philos. Mag. 97 (2017)299.

[18] S. Jitsukawa, A. Kimura, A. Kohyama, R.L. Klueh, A.A. Tavassoli, B. van der Schaaf, G.R. Odette, J.W. Rensman, M. Victoria, and C. Petersen, J. Nucl. Mater. 329-333 (2004) 39.

[19] J.M. Sanchez, F. Ducastelle and D. Gratias, Physica A 128 (1984) 334.

[20] F. Ducastelle, *Cohesion and Structure*, in : Order and Phase Stability in Alloys, vol. 3, North-Holland, Amsterdam, 1991.

[21] A. Zunger, S.H. Wei, L.G. Ferreira and J.E. Bernard, Phys. Rev. Lett. 65 (1990) 353.

[22] G. Inden and W. Pitsch, *Materials Science and Technology*, in: Phase Transformations in Materials, vol. 5, ed R. W. Cahn et al, Wiley, Weinheim, 1991, p. 497.

[23] I. Mirebeau, M. Hennion and G. Parette, Phys. Rev. Lett. 53 (1984) 687.

[24] I. Mirebeau and G. Parette, Phys. Rev. B 82 (2010) 104203.

[25] P. Erhart, A. Caro, M. Serrano de Caro and B. Sadigh, Phys. Rev. B 77 (2008) 134206.

[26] G. Bonny, D. Terentyev and L. Malerba, Scripta Mater. 59 (2008) 1193.

[27] G. Bonny, D. Terentyev and L. Malerba, J. Phase. Eq. Diff. 31 (2010) 439.

[28] G. Bonny, R.C. Pasianot, L. Malerba, A. Caro, P. Olsson and M.Yu. Lavrentiev, J. Nucl. Mater. 385 (2009) 268.

[29] T. Massalski, H. Okamoto, S. Subramaniam, L. Kacprzak, Binary alloy phase diagram, 1996.

[30] P. Olsson, C. Domain, J. Wallenius, Phys. Rev. B 75 (2007) 014110.

[31] E. del Rio, J.M. Sampedro, H. Dogo, M.J. Caturla, M. Caro, A. Caro, J.M. Perlado, J. Nucl. Mater. 408 (2011) 18.

[32] G. Bonny, R.C. Pasianot, D. Terentyev, L. Malerba, Philos. Mag. 91 (2011) 1724.

[33] G. Bonny, P. Grigorev and D. Terentyev, J. Phys. Condens. Matter 26 (2014) 485001.